The radiated acoustic pressure and time scales of a spherical bubble

Smith, Warren; Wang, Qian

DOI:
10.1088/1873-7005/abd1d0

Document Version
Peer reviewed version

Citation for published version (Harvard):
Smith, W & Wang, Q 2021, 'The radiated acoustic pressure and time scales of a spherical bubble', *Fluid Dynamics Research*, vol. 53, no. 1, 015502. https://doi.org/10.1088/1873-7005/abd1d0

The radiated acoustic pressure and time scales of a spherical bubble

W. R. Smith and Q. X. Wang

School of Mathematics, University of Birmingham, Edgbaston, Birmingham, B15 2TT, UK

E-mail: W.Smith@bham.ac.uk,Q.X.Wang@bham.ac.uk

Abstract. Numerical simulations of violent bubble dynamics are often associated with numerical instabilities at the end of collapse, when a shock wave is emitted. Based on the Keller–Miksis equation, we show that this is caused by two time scales associated with the phenomenon. Nonsingular equations are thus formed based on asymptotic expansion theory and the time derivatives of the bubble radius are shown to have algebraic singularities in the Mach number. The period of oscillation is shown to divide into two asymptotic layers: a long and short time scale. The short time scale, on which significant acoustic radiation is emitted from the bubble, has been determined to be $\bar{R}_{max}\left([\bar{p}_\infty - \bar{p}_v]/\rho c^2\right)^{1/(3\kappa)}/c$, where c is the speed of sound in the liquid, $\bar{R}_{max}$ the maximum bubble radius, ρ the liquid density, $\bar{p}_\infty$ the hydrostatic pressure of the liquid, $\bar{p}_v$ the vapour pressure of the liquid and κ the polytropic index of the bubble gas. Using the scalings for this short time scale, the radiated acoustic pressure scale has been deduced to be $\rho c^2 \bar{R}_{max}\left([\bar{p}_\infty - \bar{p}_v]/\rho c^2\right)^{1/(3\kappa)}/\mathcal{R}$, where $\mathcal{R}$ is the radial distance from the bubble centre to the point of measurement. The results are validated by comparison with experimental results.

Keywords: Bubble dynamics, Acoustic radiation, Scaling

1. Introduction

Inertial collapse of bubbles is associated with cavitation damage to pumps, turbines and propellers (Brennen 2013, Lauterborn & Kurz 2010, Leighton 1994), and the damage of an underwater explosion (Cole 1948, Klaseboer et al. 2005, Wang 2013). Inertial collapse of bubbles driven by ultrasound has wide applications in medical ultrasound (Coussios & Roy 2008, Klaseboer et al. 2007, Calvisi et al. 2008, Curtiss et al. 2013, Wang et al. 2015), sonochemistry (Suslick 1990) and ultrasonic cleaning (Ohl et al. 2006).

In this article, the bubble oscillation in a compressible liquid is analyzed based on the Keller–Miksis equation (Keller & Miksis 1980) using asymptotic expansions. The most important contribution of this article is to the understanding and interpretation of the Keller–Miksis equation. The full equation conceals the different physical balances which hold over the end of the collapse and the beginning of the expansion. The asymptotic analysis reveals precisely which balances hold and quantifies the Mach number singularity. Furthermore, we are rewarded with two explicit parameter dependencies for the short time scale associated with acoustic radiation and the radiated acoustic pressure scale.

Compressible effects in bubble dynamics are negligible for most of time but become significant for a short time period at the end of collapse, when strongly nonlinear waves or shock waves are emitted (Philipp & Lauterborn 1998, Wang 2013, Wang & Manmi 2014, Wang 2016). This happens even when the associated Mach numbers are small. The emission of shock waves and associated multiple scales in time cause numerical instabilities of the bubble dynamics at the end of collapse (Zhang et al. 2001, Lind & Phillips 2010, Lind & Phillips 2013). This also results in a challenge to predict the energy loss due to the emission of shockwaves using computational fluid dynamics (Lechner et al. 2017). Consequently, the numerical models were combined with some empirical adjustments in order to simulate multiple oscillations (Gonzalez-Avila et al. 2020). A basic question on this phenomenon is thus how long is the duration of this short time period. The short acoustic time scale obtained from the present theory can be used for setting varied time steps for the numerical simulations for non-spherical bubble dynamics.

The nonlinear oscillations of the Keller–Miksis equation are also of great interest from a mathematical perspective. The loss of energy due to acoustic radiation takes place on a much shorter time scale than the period of oscillation (Wang 2016). If this loss of energy is substantial over each cycle, then multi-layer asymptotic expansions are required to describe the oscillations of the bubble radius. This is depicted by an order one reduction in the dimensionless bubble radius between the first and second maxima in Figure 1. However, if this loss of energy is small over each cycle of oscillation, then a multi-scaled perturbation method will average the small loss of energy over the period of oscillation (Smith & Wang 2018). This is shown by a small reduction in the dimensionless bubble radius between the second and third maxima in Figure 1. If the former holds, then a region described by multi-layer asymptotic expansions

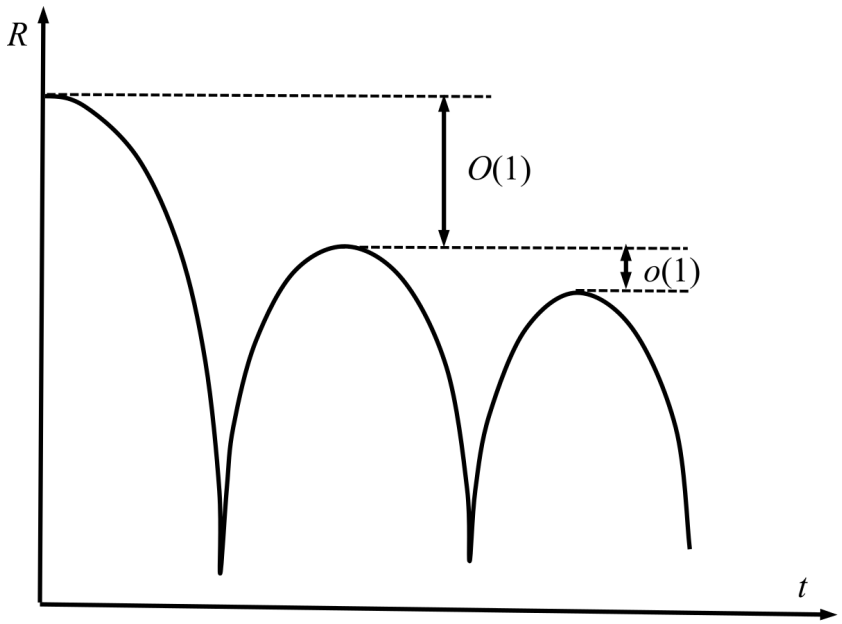

Figure 1. A schematic of the general asymptotic structure of nonlinear oscillations for the Keller–Miksis equation (5) with the dimensionless bubble radius R as a function of dimensionless time t. The multi-layer method is required when the bubble radius reduces by order one between oscillations, whereas a multi-scaled method is required when the bubble radius reduces by less than order one.

typically precedes a region described by the multi-scaled perturbation method (Smith et al. 1999). In practice, the region of multi-layer asymptotic expansions and the multi-scaled approach have an overlap in which both techniques may be applied with reasonable accuracy. Therefore, the present work extends our previous research on the multi-scaled method to more violent collapses.

The remainder of the paper is organized as follows. The mathematical model for the radiative decay of bubble oscillations is described in section 2. In section 3, nonlinear oscillations are studied with the application of multi-layer asymptotic expansions to the Keller–Miksis equation. In section 4, the theoretical solutions are firstly compared quantitatively with experimental observations which also provides quantitative validation of the acoustic radiation time scale and the bubble radius scale. The dimensional acoustic radiation time and pressure scales are then identified and compared qualitatively with experimental observations. Finally, in section 5, the results are briefly summarized.

2. Mathematical model

The radial dynamics of spherical bubbles in compressible fluids have been studied extensively for many decades. This problem was first considered in connection with an underwater explosion (Herring 1941). Keller & Kolodner (1956) and Keller & Miksis (1980) later formulated the Keller-Miksis equation for a spherical bubble using the wave

equation and the incompressible Bernoulli equation. Prosperetti & Lezzi (1986) studied the problem using the method of matched asymptotic expansions to the second order in terms of the bubble-wall Mach number. They provided a rational proof of the Keller-Miksis equation. The Keller–Miksis equation for a spherical gas bubble in a compressible liquid reads (Keller & Miksis 1980)

$$\left(1-\frac{1}{c}\frac{\mathrm{d}\bar{R}}{\mathrm{d}\bar{t}}\right)\bar{R}\frac{\mathrm{d}^2\bar{R}}{\mathrm{d}\bar{t}^2}+\frac{3}{2}\left(\frac{\mathrm{d}\bar{R}}{\mathrm{d}\bar{t}}\right)^2\left(1-\frac{1}{3c}\frac{\mathrm{d}\bar{R}}{\mathrm{d}\bar{t}}\right)=\left(1+\frac{1}{c}\frac{\mathrm{d}\bar{R}}{\mathrm{d}\bar{t}}\right)\frac{\bar{p}_l}{\rho}+\frac{\bar{R}}{\rho c}\frac{\mathrm{d}\bar{p}_l}{\mathrm{d}\bar{t}}, \tag{1}$$

where $\bar{p}_l$ is the pressure of liquid at the bubble surface and is given as follows under adiabatic conditions

$$\bar{p}_l=\bar{p}_{g0}\left(\frac{\bar{R}_{max}}{\bar{R}}\right)^{3\kappa}-\frac{2\sigma}{\bar{R}}-(\bar{p}_\infty-\bar{p}_v)-\frac{4\mu}{\bar{R}}\frac{\mathrm{d}\bar{R}}{\mathrm{d}\bar{t}},$$

in which $\bar{R}(\bar{t})$ is the spherical bubble radius at time $\bar{t}$, c the speed of sound in the liquid, $\bar{R}_{max}$ the initial maximum bubble radius, ρ the liquid density, $\bar{p}_\infty$ the hydrostatic pressure of the liquid, $\bar{p}_v$ the vapour pressure of the liquid, $\bar{p}_{g0}$ the initial pressure of the bubble gases, $\kappa>1$ the polytropic index, σ the surface tension and μ the liquid viscosity. The thermal processes typically absorb a relatively small portion of the overall energy (Akhatov et al. 2001, Szeri et al. 2003). The initial conditions are chosen when the bubble is at its maximum radius, that is

$$\bar{R}(0)=\bar{R}_{max},\qquad \frac{\mathrm{d}\bar{R}}{\mathrm{d}\bar{t}}(0)=0. \tag{2}$$

Dowling & Ffowcs Williams (1983) and Brennen (2013) derived an expression for the pressure in the far field. The radiated acoustic pressure from an oscillating bubble is given by

$$\frac{\rho}{4\pi\mathcal{R}}\frac{\mathrm{d}^2\bar{V}}{\mathrm{d}\bar{t}^2}\left(\bar{t}-\frac{\bar{r}}{c}\right), \tag{3}$$

where the radial distance, $\bar{r}$, from the bubble centre to the point of measurement is $\mathcal{R}$ ($\mathcal{R}\gg\bar{R}_{max}$) and $\bar{V}(\bar{t})$ is the time-dependent volume of the bubble.

We scale (1) using $\bar{R}=\bar{R}_{max}R$ and $\bar{t}=\bar{R}_{max}t/U$, in which

$$\Delta=\bar{p}_\infty-\bar{p}_v,\qquad U=\sqrt{\frac{\Delta}{\rho}}, \tag{4}$$

where Δ is the characteristic pressure of the liquid and U is a reference velocity. The dimensionless Keller–Miksis equation becomes

$$\left(1-\epsilon\frac{\mathrm{d}R}{\mathrm{d}t}\right)R\frac{\mathrm{d}^2R}{\mathrm{d}t^2}+\frac{3}{2}\left(\frac{\mathrm{d}R}{\mathrm{d}t}\right)^2\left(1-\frac{\epsilon}{3}\frac{\mathrm{d}R}{\mathrm{d}t}\right)=\left(1+\epsilon\frac{\mathrm{d}R}{\mathrm{d}t}\right)p_l+\epsilon R\frac{\mathrm{d}p_l}{\mathrm{d}t}, \tag{5}$$

where

$$p_l=\frac{p_{g0}}{R^{3\kappa}}-\frac{2}{WeR}-1-\frac{4}{ReR}\frac{\mathrm{d}R}{\mathrm{d}t}, \tag{6}$$

in which

$$Re=\frac{\rho U\bar{R}_{max}}{\mu},\quad We=\frac{\bar{R}_{max}\Delta}{\sigma},\quad p_{g0}=\frac{\bar{p}_{g0}}{\Delta}<1,\quad \epsilon=\frac{U}{c}$$

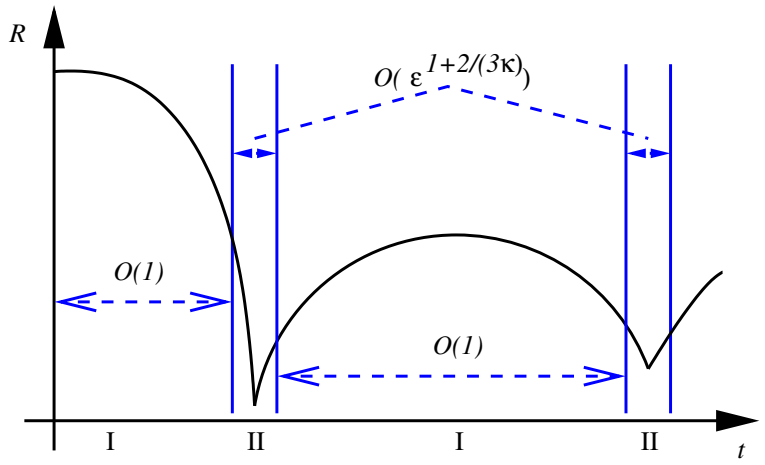

Figure 2. A schematic of the asymptotic structure of nonlinear oscillations for the Keller–Miksis equation (5), having layers I and II repeated with the time scales of $\mathcal{O}(1)$ and $\mathcal{O}(\epsilon^{1+2/(3\kappa)})$, respectively.

are the Reynolds number, the Weber number, the dimensionless initial pressure of the bubble gases and the Mach number, respectively. We define the dimensionless equilibrium radius by $R_{eq} = \bar{R}_{eq}/\bar{R}_{max}$, where $\bar{R}_{eq}$ is the dimensional equilibrium radius which is more easily measured in experiments than the dimensionless initial pressure of the bubble gases p_{g0}. If the equilibrium radius is known, we may evaluate p_{g0} via the equation

$$p_{g0} = R_{eq}^{3\kappa}\left\{1 + \frac{2}{WeR_{eq}}\right\}.$$

The initial conditions are

$$R(0) = 1, \qquad \frac{\mathrm{d}R}{\mathrm{d}t}(0) = 0. \tag{7}$$

Henceforth, we assume that the restrictions $1/Re \ll 1$ and $\epsilon \ll 1$ hold.

3. Multi-layer asymptotic expansions

We now describe the underlying physical structure of the nonlinear oscillations with significant acoustic radiation. The asymptotic structure consists of two layers in each period as shown in Figure 2.

3.1. Layer I: $t = \mathcal{O}(1)$

Firstly, we consider layer I in which $t = \mathcal{O}(1)$ and $R = \mathcal{O}(1)$. We introduce the expansion $R = R_0 + \mathcal{O}(\epsilon)$ as $\epsilon \to 0$. The radius satisfies the equation

$$R_0\frac{\mathrm{d}^2R_0}{\mathrm{d}t^2} + \frac{3}{2}\left(\frac{\mathrm{d}R_0}{\mathrm{d}t}\right)^2 = \frac{p_{g0}}{R_0^{3\kappa}} - \frac{2}{WeR_0} - 1. \tag{8}$$

Layer I remains valid until the leading-order balance changes at the end of the collapse; namely, when

$$\epsilon \left| \frac{\mathrm{d}R}{\mathrm{d}t} \right| = \mathcal{O}(1). \tag{9}$$

This criterion corresponds to the compressibility terms growing to violate the leading-order balance.

3.2. Layer II: $t = t_m + \epsilon^{1+2/(3\kappa)} t_2$

Secondly, we consider layer II. The determination of the time scale on which compressibility effects are significant (at leading order) requires the notion of a distinguished limit. In our case, the distinguished limit corresponds to a balance between inertial terms, compressibility effects and the terms for the partial pressure of the bubble gases. This balance occurs for a unique choice of the time scale and the bubble radius scale. Therefore, this limit is distinguished from all others. We find the distinguished limit by considering the scalings $t = t_m + \epsilon^{\alpha} t_2$ and $R = \epsilon^{\beta} \hat{R}$, where t_m is a time shift and α and β are to be determined. Using (5), we obtain

$$\begin{aligned} &\left(1 - \epsilon^{1+\beta-\alpha} \frac{\mathrm{d}\hat{R}}{\mathrm{d}t_2}\right) \epsilon^{2(\beta-\alpha)} \hat{R} \frac{\mathrm{d}^2 \hat{R}}{\mathrm{d}t_2^2} + \frac{3}{2} \epsilon^{2(\beta-\alpha)} \left(\frac{\mathrm{d}\hat{R}}{\mathrm{d}t_2}\right)^2 \left(1 - \frac{\epsilon^{1+\beta-\alpha}}{3} \frac{\mathrm{d}\hat{R}}{\mathrm{d}t_2}\right) \\ &= \left(1 + \epsilon^{1+\beta-\alpha} \frac{\mathrm{d}\hat{R}}{\mathrm{d}t_2}\right) p_l + \epsilon^{1+\beta-\alpha} \hat{R} \frac{\mathrm{d}p_l}{\mathrm{d}t_2}, \end{aligned}$$

in which

$$p_l = \epsilon^{-3\kappa\beta} \frac{p_{g0}}{\hat{R}^{3\kappa}} - \epsilon^{-\beta} \frac{2}{We\hat{R}} - 1.$$

The compressibility terms have now entered the leading-order physical balance, compressibility being less significant in layer I. The balance between compressibility and inertial terms requires that $1 + \beta - \alpha = 0$. As the bubble radius decreases, only the terms for the partial pressure of the bubble gases remain in the leading-order physical balance from p_l, because they increase faster than surface tension effects. The balance between inertial effects and the terms for the partial pressure of the bubble gases requires that $2(\beta - \alpha) = -3\kappa\beta$. Hence, we solve these two simultaneous equations to find $\alpha = 1 + 2/(3\kappa)$ and $\beta = 2/(3\kappa)$.

We adopt the scalings $t = t_m + \epsilon^{1+2/(3\kappa)} t_2$ and $R = \epsilon^{2/(3\kappa)} \hat{R}$ corresponding to the distinguished limit. We obtain the equation

$$\left(1 - \frac{\mathrm{d}\hat{R}}{\mathrm{d}t_2}\right) \hat{R} \frac{\mathrm{d}^2 \hat{R}}{\mathrm{d}t_2^2} + \frac{3}{2} \left(\frac{\mathrm{d}\hat{R}}{\mathrm{d}t_2}\right)^2 \left(1 - \frac{1}{3} \frac{\mathrm{d}\hat{R}}{\mathrm{d}t_2}\right) = \left(1 + \frac{\mathrm{d}\hat{R}}{\mathrm{d}t_2}\right) \hat{p}_l + \hat{R} \frac{\mathrm{d}\hat{p}_l}{\mathrm{d}t_2},$$

in which

$$\hat{p}_l = \frac{p_{g0}}{\hat{R}^{3\kappa}} - \epsilon^{2-2/(3\kappa)} \frac{2}{We\hat{R}} - \epsilon^2.$$

We introduce the expansion $\hat{R} = \hat{R}_0 + \mathcal{O}(\epsilon^{2-2/(3\kappa)})$ as $\epsilon \to 0$ to give a new leading-order balance in (5)

$$\left(1 - \frac{\mathrm{d}\hat{R}_0}{\mathrm{d}t_2}\right)\hat{R}_0\frac{\mathrm{d}^2\hat{R}_0}{\mathrm{d}t_2^2} + \frac{3}{2}\left(\frac{\mathrm{d}\hat{R}_0}{\mathrm{d}t_2}\right)^2\left(1 - \frac{1}{3}\frac{\mathrm{d}\hat{R}_0}{\mathrm{d}t_2}\right) = \left(1 + \frac{\mathrm{d}\hat{R}_0}{\mathrm{d}t_2}\right)\frac{p_{g0}}{\hat{R}_0^{3\kappa}} + \hat{R}_0\frac{\mathrm{d}}{\mathrm{d}t_2}\left(\frac{p_{g0}}{\hat{R}_0^{3\kappa}}\right). \quad (10)$$

Layer II remains valid until the leading-order balance changes during the bubble expansion phase; namely, when $R = \mathcal{O}(1)$. Equation (10) is as difficult to solve analytically as the Keller–Miksis equation (5). Matching of the asymptotic expansions in the two layers has also not been possible.

As illustrated by the following leading-order expressions

$$\frac{\mathrm{d}R}{\mathrm{d}t} \sim \frac{1}{\epsilon}\frac{\mathrm{d}\hat{R}_0}{\mathrm{d}t_2}, \qquad \frac{\mathrm{d}^2R}{\mathrm{d}t^2} \sim \frac{1}{\epsilon^{2+2/(3\kappa)}}\frac{\mathrm{d}^2\hat{R}_0}{\mathrm{d}t_2^2}, \quad (11)$$

the time derivatives of R have algebraic singularities in the Mach number ϵ. The Mach number dependence of the bubble radius has been determined in layer II and the Mach number singularity in the Keller–Miksis equation (5) has been removed by considering equation (10).

If the collapse is very intense, then new damping mechanisms must emerge in the physical situation to counter the rapid increase in the bubble velocity and acceleration revealed in (11). These new damping mechanisms are not present in the Keller–Miksis equation (5). Therefore, the Keller-Miksis equation is valid for Mach numbers ϵ in a range $\epsilon_{KM} \ll \epsilon \ll 1$, where ϵ_{KM} is a constant Mach number. Although this limitation of the Keller–Miksis equation for the most intense collapse has been widely discussed in the literature, the evidence provided by (11) is new and compelling.

4. Numerical results

4.1. Validation

Equation (10) is a simplified model for the final stages of the bubble collapse and rebound. In order to validate the simplifications in (10), comparisons with experimental observations are sought. Our approach is to solve the Keller–Miksis equation (5) with the fourth order Runge–Kutta method in layer I. The choice of the Keller–Miksis equation (5) rather than (8) is equivalent to solving the problem in layer I to all orders in ϵ. We continue as described until criterion (9) applies in the form

$$\epsilon\left|\frac{\mathrm{d}R}{\mathrm{d}t}\right| > 0.1. \quad (12)$$

Our solution approach is to use patching based on the criterion (12); that is, the values of radius and its first derivative from layer I are used as the initial conditions for layer II. The layer II equation (10) is then solved with the fourth order Runge–Kutta method until the condition (12) no longer holds. This procedure may be repeated on the second oscillation if necessary.

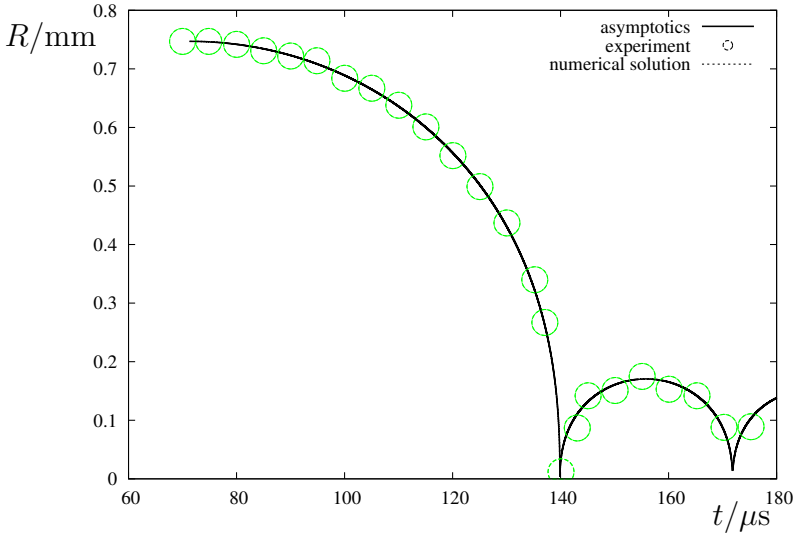

Figure 3. Comparison of the time histories of a spherical bubble using asymptotic expansions for the Keller–Miksis equation (5)-(6), experimental results (Kröninger et al. 2010) and full numerical solution of the Keller–Miksis equation (5)-(6). In this experiment, short pulses of laser light were focussed into water. The asymptotic expansions employs the solution to (10) and the criterion (12). The parameter values used in the calculations are the Reynolds number $Re \approx 7.5 \times 10^3$, the Weber number $We \approx 1.04 \times 10^3$, $p_{g0} \approx 7.44 \times 10^{-5}$ and the Mach number $\epsilon \approx 0.00667$.

We consider the evolution of (nearly) spherical bubbles obtained by focussing short pulses of laser light into water (see Figure 5 of Kröninger et al. (2010)). The following values are adopted following the experimental conditions $\Delta = 1.01 \times 10^5 \text{kgm}^{-1}\text{s}^{-2}$, $\sigma = 0.0725\text{Nm}^{-1}$, $\kappa = 1.33$, $\mu = 0.001\text{Pas}$, $c = 1500\text{ms}^{-1}$, $\rho = 998\text{kgm}^{-3}$, $\bar{R}_{max} = 747\mu\text{m}$ and $\bar{R}_{eq} = 69\mu\text{m}$. From the above parameters, we deduce that the Reynolds number $Re \approx 7.5 \times 10^3$, the Weber number $We \approx 1.04 \times 10^3$, the Mach number $\epsilon \approx 0.00667$ and $p_{g0} \approx 7.44 \times 10^{-5}$. In order to validate the analysis of the final stages of the bubble collapse and rebound in layer II, a numerical solution is obtained for these parameter values. We note that there are no unknown parameters to fit with the experimental results. Figure 3 compares the asymptotic solution for the bubble radius with the experimental results and the full numerical solution, the agreement being remarkable. The condition (12) is satisfied during the first minimum in Figure 3, but not the second or subsequent minima.

Experimental observations of the final stages of the collapse phase and rebound of the bubble have been captured using high-speed photography (see Figure 29 of Lauterborn & Kurz (2010)). These experimental results allow a direct comparison with the analysis in layer II. The experimental conditions are identical to Figure 5 of Kröninger et al. (2010) except that $\bar{R}_{max} = 1.1\text{mm}$ and $\bar{R}_{eq}$ is not specified. With the above parameters, we deduce that the Reynolds number $Re \approx 1.1 \times 10^4$, the Weber number $We \approx 1.5 \times 10^3$ and the Mach number $\epsilon \approx 0.00667$. The dimensionless initial pressure of the bubble gases $p_{g0} \approx 1.5 \times 10^{-4}$ is chosen to fit with the experimental

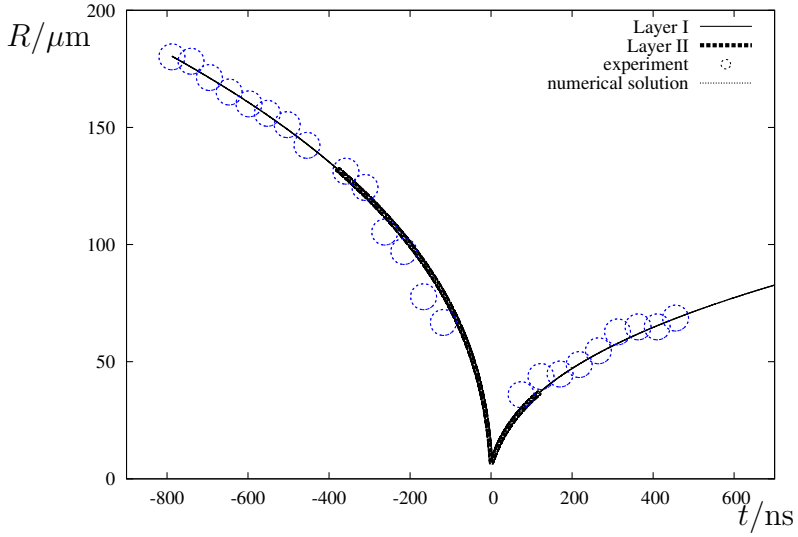

Figure 4. Comparison of the time histories of a spherical bubble in the neighbourhood of the minimum using the two layers for the Keller–Miksis equation (5)-(6), experimental results (Lauterborn & Kurz 2010) and full numerical solution of the Keller–Miksis equation (5)-(6). In this experiment, the bubble collapse was captured using high-speed photography. The asymptotic expansions employs the solution to (10) and the criterion (12). The parameter values used in the calculations are the Reynolds number $Re \approx 1.1 \times 10^4$, the Weber number $We \approx 1.5 \times 10^3$, $p_{g0} \approx 1.5 \times 10^{-4}$ and the Mach number $\epsilon \approx 0.00667$.

results. In this comparison, we follow Lauterborn & Kurz (2010) and take the initial conditions to be $R(t_0) = 180\mu$m and $\dot{R}(t_0) = -96.2\text{ms}^{-1}$ with $t_0 = -788$ns in order to move the bubble collapse to the origin. These initial conditions start in layer I shortly before the condition (12) is satisfied. Figure 4 compares the bubble radius obtained from the asymptotic solution with the experimental results and the full numerical solution, the agreement being excellent. In Figure 4, layer II begins at -379ns during the collapse and ends at 119ns during the expansion. The errors made in layer II, which are of the order of $\epsilon^{2-2/(3\kappa)}$, may not be discerned.

4.2. Acoustic radiation time scale

The dimensional acoustic radiation time scale, $\bar{t}_a$, is the time scale on which the compressibility effects are significant at leading order; that is, the time scale in layer II. Using the analysis in layer II, we obtain

$$\bar{t}_a = \frac{\bar{R}_{max}}{U}\epsilon^{1+2/(3\kappa)} = \frac{\bar{R}_{max}}{c}\left(\frac{[\bar{p}_\infty - \bar{p}_v]}{\rho c^2}\right)^{1/(3\kappa)}. \tag{13}$$

This acoustic time scale is compatible with numerical solutions in layer II and the experimental results. Therefore, Figures 3 and 4 have already provided quantitative validation for this acoustic time scale. For the experimental results plotted in Figures 3 and 4, the acoustic time scales are 40ns and 60ns, respectively.

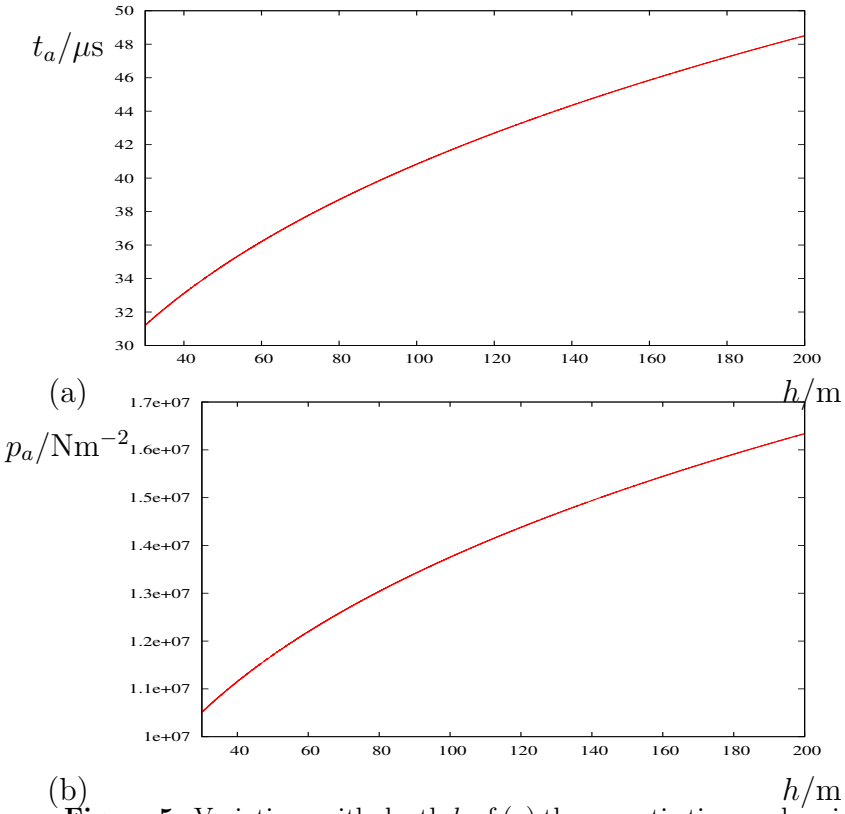

Figure 5. Variations with depth h of (a) the acoustic time scale using (13) and (b) the radiated acoustic pressure scale (14). The data correspond to $\kappa = 1.25$, $c = 1500\text{ms}^{-1}$, $\rho = 998\text{kgm}^{-3}$, $\mathcal{R} = 10\text{m}$ and $\bar{R}_{max} = 0.47\text{m}$.

Figure 67 of Lauterborn & Kurz (2010) plots the experimental results for the width (full width at half maximum) of the first collapse pressure pulse as a function of the maximum bubble radius (R_{max}). The dependence is linear for smaller bubbles as predicted by (13), but the growth slows for larger bubbles.

4.3. Radiated acoustic pressure scale

The dimensional radiated acoustic pressure scale, $\bar{p}_a$, may be deduced by using the expression (3) and the time scale and bubble radius scale in layer II. We obtain

$$\bar{p}_a = \frac{\rho c^2 \bar{R}_{max}}{\mathcal{R}} \left(\frac{[\bar{p}_\infty - \bar{p}_v]}{\rho c^2} \right)^{1/(3\kappa)} . \tag{14}$$

Figures 3 and 4 have already provided quantitative validation for the scales used in calculating the acoustic pressure scale. The experiments in Figure 6 of Isselin et al. (1998) and Figure 66 of Lauterborn & Kurz (2010) have previously found a linear dependence of the first collapse pressure on the maximum bubble radius $\bar{R}_{max}$.

We next consider a tetryl charge of 0.249kg detonated 91.44m below the water surface (Cole 1948). The following values for gas bubbles in water are adopted following the experimental conditions $\kappa = 1.25$, $c = 1500\text{ms}^{-1}$, $\rho = 998\text{kgm}^{-3}$ and $\bar{R}_{max} = 0.47\text{m}$. With the above parameters and the radial distance from the bubble centre to the point

of measurement is $\mathcal{R} = 10$m, we predict the acoustic time scale and the radiated acoustic pressure scale as a function of depth in Figure 5.

5. Summary and conclusions

In summary, a theoretical study has been carried out to investigate the acoustic decay of nonlinear oscillations of a spherical bubble in a compressible inviscid fluid, using the Keller–Miksis equation. The acoustic radiation is essential only during the short period at the end of the collapse and at the beginning of the expansion. The Keller–Miksis equation is shown to have an algebraic singularity in the Mach number during this short period. Two important results have been obtained: the short time scale associated with acoustic radiation and the radiated acoustic pressure scale. We note that the dependence of both the acoustic radiation time and pressure scales on the hydrostatic pressure of the liquid should be of great interest in deep water applications. The present theory has the potential to be developed for nonspherical bubbles. This will be valuable to overcome the numerical instabilities associated the violent collapse of nonspherical bubbles.

References

Akhatov I, Lindau O, Topolnikov A, Mettin R, Vakhitova N & Lauterborn W 2001 *Phys. Fluids* **13**, 2805.

Brennen C E 2013 *Cavitation and Bubble Dynamics* Cambridge University Press.

Calvisi M L, Iloreta J I & Szeri A J 2008 *J. Fluid Mech.* **616**, 63–97.

Cole R H 1948 *Underwater Explosions* Princeton University Press, Princeton.

Coussios C C & Roy R A 2008 *Annu. Rev. Fluid Mech.* **40**, 395–420.

Curtiss G A, Leppinen D M, Wang Q X & Blake J R 2013 *J. Fluid Mech.* **730**, 245–272.

Dowling A P & Ffowcs Williams J E 1983 *Sound and Sources of Sound* Ellis Horwood Ltd and John Wiley and Sons.

Gonzalez-Avila S R, van Blokland A C, Zeng Q & Ohl C D 2020 *J. Fluid Mech.* **884**, A23.

Herring C 1941 The theory of the pulsations of the gas bubbles produced by an underwater explosion Technical Report 236 US Nat. Defence Res. Comm. Report.

Isselin J C, Alloncle A P & Autric M 1998 *J. Appl. Phys.* **84**, 5766–5771.

Keller J B & Kolodner I I 1956 *J. Appl. Phys.* **27**, 1152–1161.

Keller J B & Miksis M 1980 *J. Acoust. Soc. Am.* **68**, 628–633.

Klaseboer E, Fong S W, Turangan C K, Khoo B C, Szeri A J, Calvisi M L, Sankin G N & Zhong P 2007 *J. Fluid Mech.* **593**, 33–56.

Klaseboer E, Hung K C, Wang C, Wang C W, Khoo B C, Boyce P, Debono S & Charlier H 2005 *J. Fluid Mech.* **537**, 387–413.

Kröninger D, Köhler K, Kurz T & Lauterborn W 2010 *Exp. Fluids* **48**, 395–408.

Lauterborn W & Kurz T 2010 *Rep. Prog. Phys.* **73**, 106501.

Lechner C, Koch M, Lauterborn W & Mettin R 2017 *J. Acoust. Soc. Am.* **149**, 3649.

Leighton T G 1994 *The Acoustic Bubble* Academic Press, London.

Lind S J & Phillips T N 2010 *J. Non-Newtonian Fluid Mech.* **165**, 852–865.

Lind S J & Phillips T N 2013 *Phys. Fluids* **25**, 022104.

Ohl C D, Arora M, Ikink R, de Jong N, Versluis M, Delius M & Lohse D 2006 *Biophys. J.* **91**, 4285–4295.

Philipp A & Lauterborn W 1998 *J. Fluid Mech.* **361**, 75–116.

Prosperetti A & Lezzi A 1986 *J. Fluid Mech.* **168**, 457–478.

Smith W R, King J R, Tuck B & Orton J W 1999 *IMA J. Appl. Math.* **63**, 1–36.

Smith W R & Wang Q X 2018 *J. Fluid Mech.* **837**, 1–18.
Suslick K S 1990 *Science* **247**, 1439–1445.
Szeri A J, Storey B D, Pearson A & Blake J R 2003 *Phys. Fluids* **15**, 2576–2586.
Wang Q X 2013 *Phys. Fluids* **25**, 072104.
Wang Q X 2016 *J. Fluid Mech.* **797**, 201–230.
Wang Q X & Manmi K 2014 *Phys. Fluids* **26**, 032104.
Wang Q X, Manmi K & Liu K 2015 *Interface Focus* **5**, 20150018.
Zhang Y L, Yeo K S, Khoo B C & Wang C 2001 *J. Comput. Phys.* **166**, 336–360.